

High-Energy Electron Scattering and Nuclear Structure Determinations*†‡

R. HOFSTADTER, H. R. FECHTER, AND J. A. MCINTYRE

Department of Physics and W. W. Hansen Laboratories, Stanford University, Stanford, California

(Received June 26, 1953)

Electrons of energies 125 and 150 Mev are deflected from the Stanford linear accelerator and brought to a focused spot of dimensions 3 mm×15 mm at a distance of 9 feet from a double magnet deflecting system. The focus is placed at the center of a brass-scattering chamber of diameter .20 inches. Thin foils are inserted in the chamber and elastically-scattered electrons from these foils pass through thin aluminum windows into the vacuum chamber of a double focusing analyzing magnet of the inhomogeneous field type. The energy resolution of the magnet has been

about 1.5 percent in these experiments. This resolution is enough to separate clearly hydrogen or deuterium elastic peaks from carbon peaks in the same scattering target. The energy loss in the foils is readily measurable. In the case of light nuclei, e.g., H, D, Be, C, the shift of the peak of the elastic curve as a function of scattering angle indicates the recoil of the struck nucleus. Relative angular distributions are measured for Be, Ta, Au, and Pb. It is possible to interpret these data in terms of a variable charge density within the nucleus.

I. INTRODUCTION

IN a recent publication¹ it was suggested that the gold nucleus does not have a sharp boundary. In this paper it is proposed to amplify this statement and to present data on other nuclei which tend to bear out this conclusion.

Guth² first pointed out that the finite size of the nucleus should produce large deviations from the expected scattering resulting from a point charge whenever the electron wavelength is of the order of nuclear dimensions. In principle, such deviations might be wholly or partially ascribed to departures from the Coulomb law of electric interaction at very small distances. In the following discussions it will be assumed that the Coulombian interaction holds at small distances and that the departures, if any, from point charge scattering are assignable to the finite dimensions of the nuclear charge distribution.

Other authors have subsequently considered the problem of the finite size of nuclei in relation to scattering experiments.³⁻⁸ Parzen, Smith, and Schiff have dealt with energies of the order of 100 Mev and higher, while the other authors have been concerned mainly with lower energies. Parzen has made an exact calculation at a high energy (100 Mev). Unfortunately, a

numerical error crept into Parzen's work and his published scattering curve cannot be considered reliable.⁹ For nuclei having a uniform or spherical shell distribution of charge all Born approximation calculations predict maxima and minima in the angular distribution. These features are essentially diffraction phenomena and are similar to the observations in electron diffraction studies of atoms. The first Born approximation^{2,4,7} for these models produces the first of a set of zeros in the angular intensity pattern at those angles where

$$qa \cong 3.5, \quad (1)$$

$$q = (4\pi/\lambda) \sin(\theta/2), \quad (2)$$

in which λ is the wavelength of the incident electrons and "a" is the rms value of the nuclear radius, calculated with the charge as the weighting factor. Yennie *et al.*¹⁰ have shown that for a uniform model the exact calculation provides a result in which the first diffraction minimum is practically washed out and the second and third less pronounced than in the Born approximation but approximately in the same angular positions. Experimental indications of a deviation from point charge scattering have been found by Lyman, Hanson, and Scott¹¹ at an electron energy of 15.7 Mev. $\lambda = \lambda/2\pi$ is, in this case, of the order of 1.25×10^{-12} cm and, if one uses a conventional radius for gold ($R = 8.1 \times 10^{-13}$ cm, $a = 6.3 \times 10^{-13}$ cm), qa is found to be close to or less than unity. Thus, no maxima or minima are to be expected in the experiment of Lyman *et al.*, although marked deviations in the angular distribution were expected and, in fact, found. The experimental data proved to be consistent with a uniformly charged model of the nucleus in which

$$R = r_0 A^{1/3}, \quad (3)$$

where r_0 was 1.45×10^{-13} cm. In gold a twenty percent smaller radius gave a very slightly improved fit of the

* This work was initiated and aided at all stages by a grant from the Research Corporation. It was supported by the joint program of the U. S. Office of Naval Research and the U. S. Atomic Energy Commission. In the latter stages of the work, support has been received from the Office of Scientific Research, Air Research, and Development Command.

† This material was presented in part at the April 29, 30-May 1, 1953 Meeting of the American Physical Society in Washington, D. C.

‡ Portions of the theoretical interpretation were revised in proof. ¹Hofstadter, Fechter, and McIntyre, *Phys. Rev.* **91**, 422 (1953).

²E. Guth, *Wiener Anzeiger Akad. Wissenschaften* No. 24, 299 (1934).

³G. Parzen, *Phys. Rev.* **80**, 261 (1950); **80**, 355 (1950).

⁴L. R. B. Elton, *Proc. Phys. Soc. (London)* **A63**, 1115 (1950); **65**, 481 (1952); *Phys. Rev.* **79**, 412 (1950).

⁵H. Feshbach, *Phys. Rev.* **84**, 1206 (1951); **88**, 295 (1952).

⁶L. K. Acheson, *Phys. Rev.* **82**, 488 (1951).

⁷J. H. Smith, Ph.D. thesis, Cornell University, 1951 (unpublished).

⁸L. I. Schiff, following paper, *Phys. Rev.* **93**, 988 (1953).

⁹G. Parzen (private communication). The error was first found by Elizabeth Baranger (private communication).

¹⁰Yennie, Wilson, and Ravenhall have recently recalculated the exact scattering at high energies (private communication).

¹¹Lyman, Hanson, and Scott, *Phys. Rev.* **84**, 626 (1951).

data. Lyman *et al.* have noted that the smaller radius in gold might indicate a more dense packing of protons in the interior of the nucleus. A suggestion of this type had been made previously by Born and Yang.¹²

The experiments to be described below were intended to search for possible clear-cut signs of nuclear finite dimensions and by this means to find nuclear radii and charge distributions.

II. APPARATUS

Only the main features of the experimental equipment will be described at this time. Figure 1 shows the principal experimental arrangement. A monoenergetic group of electrons is deflected by a system of two magnets from the main beam of the Stanford linear accelerator.¹³ The first magnet bends and disperses the beam and the second magnet bends in a reverse direction and refocuses the spread-out beam. A slit at position *S* determines the width of the accepted energy band, in this case about 3 percent. The initial width of the beam entering the first magnet is determined by the collimator *C*, in this case a $\frac{1}{4}$ -inch cylindrical hole in a uranium block 1.0-inch long. A well focused beam emerges from the second magnet and closes to a small spot 9 feet from the second magnet. The position of the spot is accurately given by simple first-order calculation of trajectories. The size of the spot is approximately 1-mm high and 3-mm wide for a $\frac{1}{16}$ -inch collimator and 3 mm \times 15 mm for a $\frac{1}{4}$ -inch collimator. The beam has extremely little divergence because of the 9.0-foot focal distance and small slit *S* used (0.75). As many as 2×10^8 electrons per pulse have been measured in the focused beam, sixty pulses occurring per second, each lasting about 0.5 microsecond. The beam is quite free of any gamma rays produced at the collimator and slit because of the double deflection. The beam stopper *B* prevents gamma rays produced at *C* from traveling down the accelerator tube and producing unwanted background in the experimental area.

The focused beam is directed towards a scattering target, usually a thin foil of any one of various materials. The scattering target is placed at the center of a brass scattering chamber of diameter twenty inches and twelve inches high. The scattering chamber is built in the form of a large bell-jar which can be detached readily from the main base plate. The whole deflection system and scattering chamber are evacuated to high vacuum. The base of the scattering chamber contains electrical lead-in connections and provisions for mounting and internally moving one or more scintillation counters on a large ring gear whose position is controllable remotely. A thin aluminum window (0.006 in.) stretches around the chamber from about -150° to 150° over a vertical distance of three inches. Scattered electrons from the target emerge from the chamber

¹² M. Born and L. M. Yang, *Nature* **166**, 399 (1950).

¹³ Among those mainly responsible for this system are Dr. J. A. McIntyre and Dr. W. K. H. Panofsky.

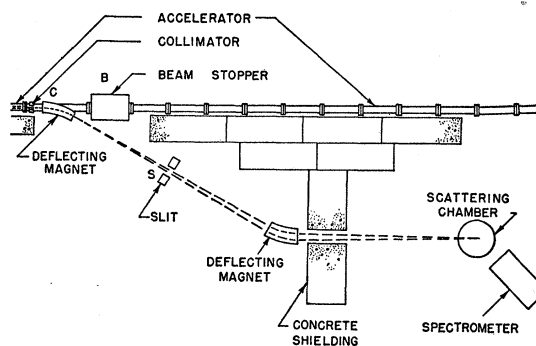


FIG. 1. The experimental arrangement of the electron-scattering system.

through the aluminum window and pass through about one inch of air before reaching the entrance port of the vacuum chamber of the analyzing magnet *M*. The C-shaped vacuum chamber lies between the shaped pole pieces of the inhomogeneous field magnet. The entrance and exit ports of the vacuum chamber are fitted with 3-mil aluminum windows. The magnet *M* is similar to the design of Snyder *et al.*,¹⁴ weighs about two and a half tons and has a mean radius of curvature of 16 inches. It is located on the movable platform of a modified twin 40-mm anti-aircraft gun mount kindly lent us by the U. S. Navy, with the cooperation of the U. S. Office of Naval Research.¹⁵ The magnet is of the double focusing variety and employs an inhomogeneous field of index $n = \frac{1}{2}$. Fields up to 12 or 13 kilogauss have been obtained and maintained over long periods of time without excessive heating. The field is usually maintained constant by manual regulation of the current.

A rotatable foil-holder that can be remotely controlled is now being installed in the scattering chamber. The experiments to be described were carried out with a substitute foil-holder which could be rotated and raised or lowered. The raising or lowering operation was remote, but the rotation was not. The holder could accommodate two foils at a time.

After the scattered electrons are analyzed in the magnet they leave the vacuum chamber and are collimated by a $\frac{1}{2}$ -in. cylindrical hole in a lead block $2\frac{1}{2}$ inches long. Behind this collimator a conical Čerenkov counter, four inches long, detects the electrons admitted by the collimator. The Čerenkov counter is made of highly polished lucite and is one inch at the narrow input end and 1.5 in. at the output end where the lucite is coupled via heavy silicone oil to a 6292 Dumont

¹⁴ Snyder, Rubin, Fowler, and Lauritsen, *Rev. Sci. Instr.* **21**, 852 (1950); C. W. Li, Ph.D. thesis, California Institute of Technology, 1951 (unpublished).

¹⁵ The gun mount was modified and machined most capably by the machine shop of the Mare Island Shipyard of the U. S. Navy. We are very grateful to the officers and civilians of the yard for the excellent job done. The U. S. Office of Naval Research very kindly helped us make the necessary arrangements with the shipyard.

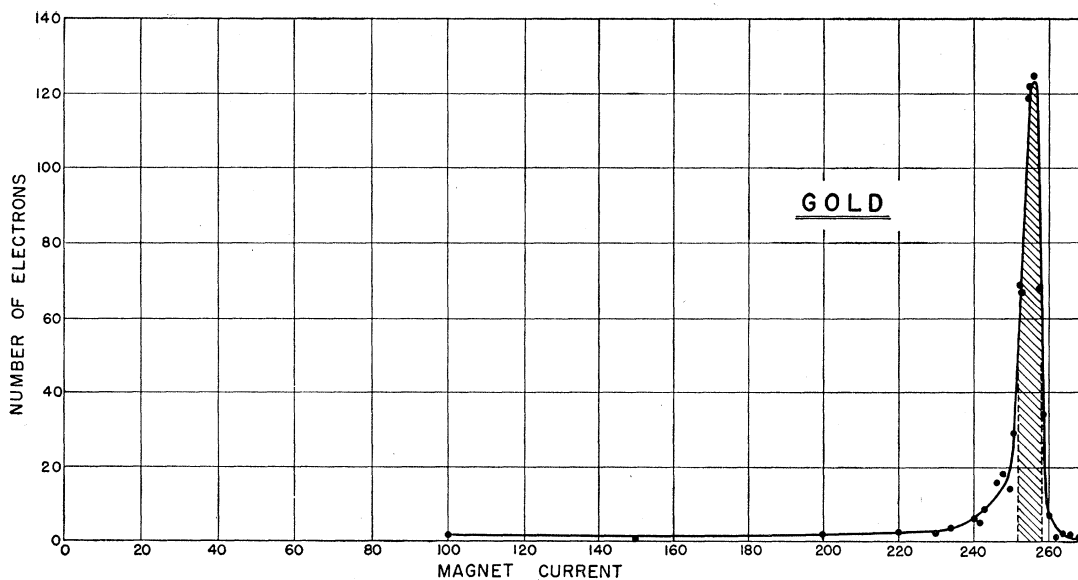


FIG. 2. An elastic-scattering curve in gold taken at 125 Mev, at a scattering angle of 35° , and with a 2-mil foil set at 45° with respect to the beam. The shaded portion of the peak shows the fraction of electrons counted in an individual peak setting. The abscissa is proportional to electron energy.

Photomultiplier. The pulses from the photomultiplier are amplified in an Elmore model 501 amplifier and fed to a gated scaler (gate 12 microseconds long) and also to an oscilloscope viewed by a monitor photomultiplier which has been made to act as a counter.¹⁶ Both counters are gated by the main trigger signal of the linear accelerator. The biases against which both counters operate are adjusted so that the two agree on number of counts. Good plateaus in counting rates are thus obtained. An effort is made to count not more than one count a second so that pileup and loss of counts may be avoided. A large lead shield surrounds the Čerenkov counter and photomultiplier and has greatly helped in avoiding background troubles.

The main beam passing through the scattering target is monitored by a helium-filled ionization chamber designed by W. C. Barber of this laboratory. Dr. Barber has kindly calibrated and tested the chamber with 25-Mev electrons and has verified that it does not saturate under beam intensities up to 2×10^8 electrons per pulse, where a pulse lasts about 0.3 microsecond, and where the beam is about 2 cm^2 or larger on entering the chamber. Under the conditions of the experiments here reported the ion chamber does not saturate. The output of the chamber is brought to a charge integrator of a conventional type.

The deflecting magnets are presently stabilized by an electronic regulator to better than one part in a thousand. The analyzing magnet is manually controlled by an operator who reads the voltage across a shunt in series with the current. A Rubicon potentiometer is used to read the shunt voltage. With careful

control the analyzing magnet current may be maintained constant between limits of ± 0.1 percent during a run of 10 minutes duration.

The magnet has been calibrated by using the known energy of the Am^{241} α particles and by measurement of the magnetic field at the center of the magnet.

The angular position of the magnet on the gun mount stand is controlled remotely and measured by a combination of high and low speed selsyn indicators. The error in determining position is less than 0.1° .

III. EXPERIMENTAL PROCEDURE

Because of the temporary nature of the target holder the scattering foils were not rotated during the angular runs. This procedure has the advantage that one always uses the same region of the scattering foil provided that the beam spot does not shift during a run. When setting the analyzing magnet from one side of zero to the other, it is of course necessary to rotate the target foil and this was done. Also when points beyond 90° were examined, the foil was rotated to a new fixed position. A typical setting of the foil for a run between 35° and 90° was with foil plane at 45° with respect to the beam. The lineup of the beam was carefully carried out at the beginning of each run by a photographic method.

At a given angular position of the analyzing magnet an "elastic curve" can be obtained by measuring the total number of counts per unit integrated beam for various settings of the magnetic field. The magnetic field settings are assumed to be proportional to the magnet currents and the former are also proportional to the electronic momenta. For these high energies, the currents are therefore also proportional to the electronic energies. Typical elastic curves so obtained are shown in

¹⁶ R. Hofstadter and J. A. McIntyre, *Rev. Sci. Instr.* **21**, 52 (1950).

Figs. 2, 3, 4, and 5. The abscissa on these curves is proportional to the magnet current, and in all cases except Fig. 2 the zero of abscissa is far off to the left of the ordinate axis. The curve of magnetic field against magnet current shows little saturation in the region here investigated¹⁴ (about 100 amperes).

The elastic curves show typical bremsstrahlung tails on the low-energy side and sharper cutoffs on the high-energy side, as expected. Figure 2 shows the appearance of an elastic curve for gold and indicates also the fraction of electrons collected in individual peak settings. Figure 3 shows a typical displacement between the peak of the main beam and that of the transmitted beam at zero degrees, the difference being the result of the energy loss in the gold foil (2-mils thick). Figures 3 and 4 show that the elastic curves have the same appearance at angular settings of 0°, 35°, and 70° and presumably, therefore, at other angles. Figure 5 and Figs. 1 and 2 of our earlier communication¹ show that the elastic curves of hydrogen and deuterium in polyethylene as well as beryllium shift with the angular position. This shift has been explained¹ by the recoil of the struck nucleus (H, D, Be, C). With improved resolution this recoil shift will permit scattering measurements to be made on unseparated isotopes in the same foil and also with the elements of compounds. In the case of Ta, Au, and Pb the recoil shift is too small to be observed at the present time. In those cases in which the elastic curves have the same appearance at all angles, it is sufficient to measure the total elastic yield at a given angle by an average of two measurements taken at positions on

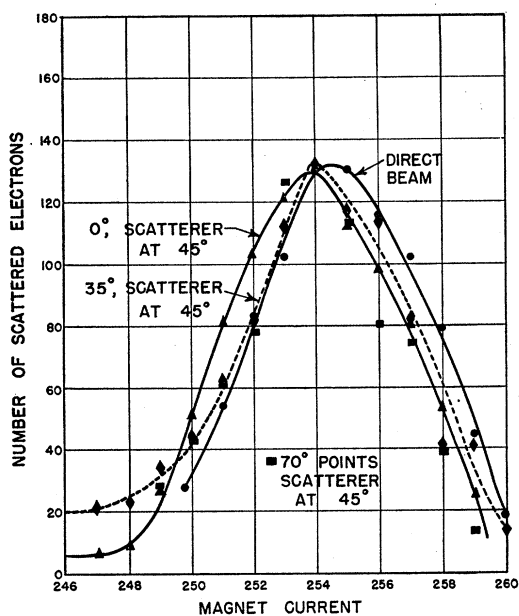


FIG. 3. Elastic-scattering curves for a 2-mil gold foil at 125 Mev. The foil was placed at 45° with respect to the beam. The abscissa is proportional to electron energy. Some of the curves were observed with a CsBr(Tl) detector by a dc method and have higher residual backgrounds (directly and indirectly the result of neutrons) than the normal Cerenkov detector curves.

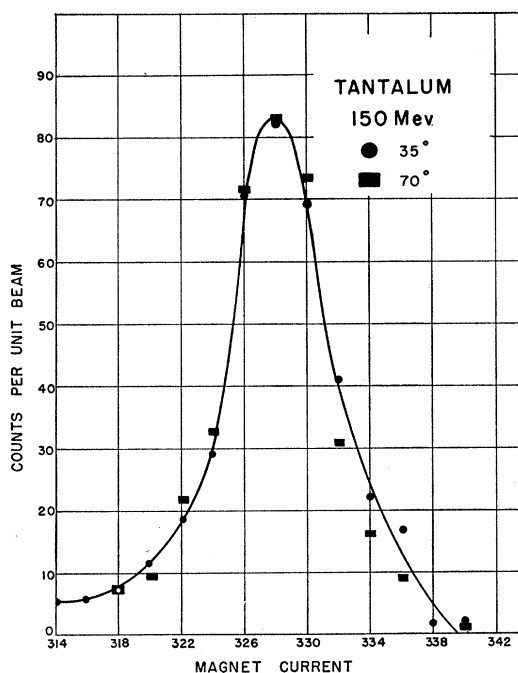


FIG. 4. Elastic-scattering curves in tantalum at 150 Mev. The data at 35° and 70° are essentially identical when normalized to the same peak value. The foil was 2.6 mils thick and was placed at 30° with respect to the direction of the beam.

either side of the peak, for example, at abscissas 326 and 330 in Fig. 4 for tantalum. All angular distributions have been measured in this way. Measurements in light elements, for example, Be or C, must be taken at the positions of the shifted peaks. Figure 6 shows how the Be elastic curves shift with angular position. In fact, in Be the elastic curve changes in appearance as well as shifts with change in angular position. The peculiar curve in Be at 90° requires further investigation. It is possible that inelastic scattering may be observed in such light elements at large angles.

The shift of the peak in Be is the result not only of the recoil energy but also of the energy loss of the incoming and outgoing electrons in the target foil. At a scattering angle of 45°, and a target setting of 45° with respect to the beam, the average energy loss in the 50-mil beryllium target is 0.49 Mev, and the recoil shift is 0.46 Mev. At 70° the corresponding figures are 0.51 Mev and 1.04 Mev, and at 90° they are 0.58 Mev and 1.58 Mev. The expected shifts relative to 35° are therefore 0.60 Mev for 70° and 1.21 Mev for 90°. The observed relative shifts are 0.60 ± 0.20 Mev and 1.20 ± 0.20 Mev and are in good agreement with the calculations. Similarly, good agreement has been obtained for the hydrogen and deuterium shifts. In fact the H, D shifts relative to carbon or some other standard may be used to measure the energy of the incident beam. With the present resolution and the accompanying experimental error in measuring the shifts, the calculated beam energy is of the order of 140 ± 20 Mev while the

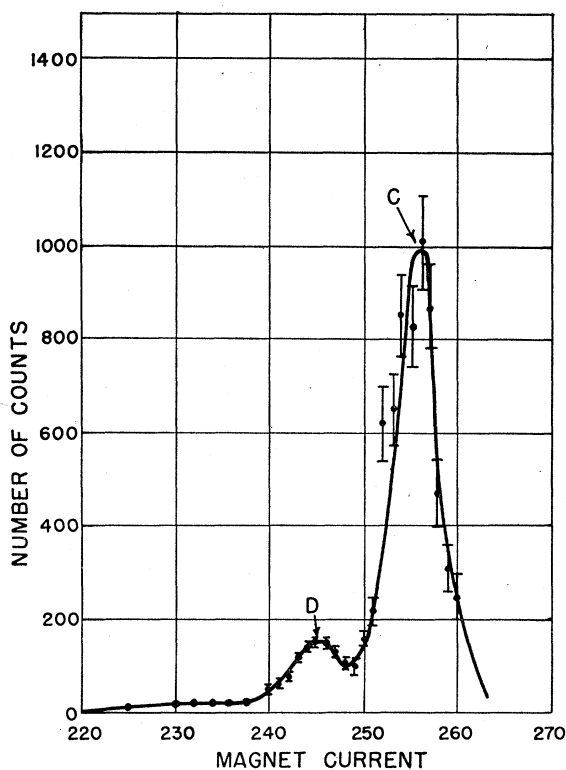


FIG. 5. An elastic curve at 125 Mev, showing the deuterium and carbon peaks observed in deuterated polyethylene at a scattering angle of 65° .

value obtained by calibration with alpha particles gives a value of 125 ± 5 Mev. Obviously, the method can be refined.

A further check on the internal consistency of the scattering data is obtained by comparison of the ratio of the areas under the carbon and hydrogen or deuterium peaks in Fig. 1 of this paper and also in Fig. 2 of reference 1. The ratio in Fig. 5 is $\sigma_C/\sigma_D = 14 \pm 5$ and

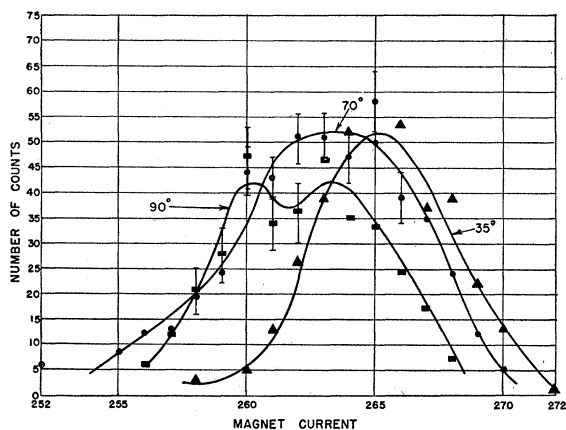


FIG. 6. Elastic curves in Be at 125 Mev at 35° , 70° , and 90° , observed with a 50-mil scattering target. The elastic peak shifts to lower energies at larger angles of scattering and also broadens as it shifts.

for Fig. 2 of reference 1 the ratio $\sigma_C/\sigma_H = 20 \pm 5$, where σ_C , σ_H , σ_D , are the respective cross sections. The accuracy of these measurements is not high because of the carbon bremsstrahlung background which must be subtracted from the H or D peaks. An average of the two results gives 17 which is close to the ratio, $Z_C^2/2(Z_{H,D})^2 = 18$, of the scattering from carbon and hydrogen or deuterium in polyethylene. Again, with better resolution this measurement of relative areas can be greatly improved, and, in fact, this method suggests itself for measuring the hydrogen and deuterium scattering cross sections relative to carbon as a standard.

To check the over-all behavior of the scattering measurements, two tests have been made: (1) the scattering

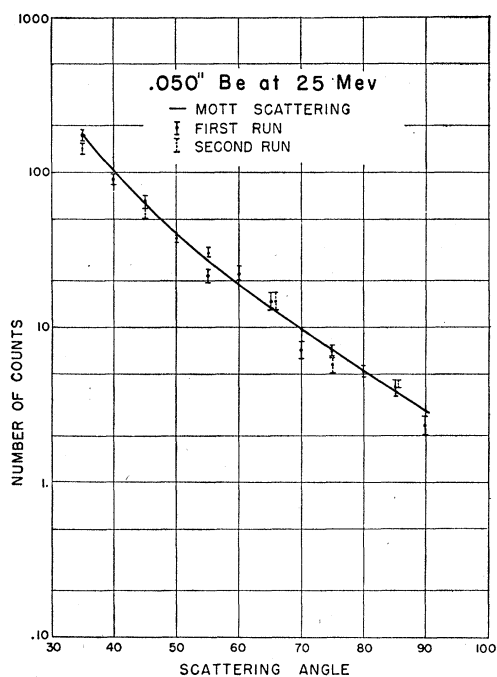


FIG. 7. The angular distribution of electrons scattered from a Be target, 50 mils thick, at 25 Mev. The target plane was at 45° with respect to the beam. The Mott curve for a point charge is shown. Arbitrary normalization is made at 35° .

of Be has been examined in the angular range 35° – 90° at 25 ± 2 Mev, and (2) the scattering from a gold foil of $\frac{1}{4}$ -mil thickness has been studied in the same angular range at 25 Mev. In case (1), because of the relatively low energy, the Be nucleus may be approximated by a point charge and the exact calculations of Feshbach⁶ and Parzen⁸ for a point charge may be compared with the experimental data. In case (2) the observed angular distribution may be compared with the data of Lyman *et al.* at 15.7 Mev.

Figure 7 shows the Be data at 25 Mev using a 50-mil foil. The data are in excellent agreement with the accurate calculations and also with the Mott formula, which for low Z 's is very close to the accurate formulas.

Figure 8 shows the data for gold found at 25 Mev

with a $\frac{1}{4}$ -mil foil. The observed curve is seen to lie above the Mott curve, just as in the work of Lyman *et al.*¹¹ Our data show slightly less rise relative to the Mott curve as compared with the data of Lyman *et al.*, but this is to be expected, to some extent, because of the higher energy and therefore the shorter wavelength relative to nuclear size. On the whole, the agreement is better than might have been anticipated, since our windows were not designed for energies as low as 25 Mev. It is gratifying that the results for Be and Au at 25 Mev are so well in accord with expectation.

To check whether some systematic error might be prejudicing results on one side of zero preferentially the data for tantalum at 150 Mev have been observed on both sides of zero. Figure 9 shows the data and shows there is nothing special on either side. The data agree very well, and, in fact, the only point seriously off is at 80° on the left side where there was a steel supporting post blocking out part of the solid angle seen by the magnet chamber.

It is also pleasing that the background counting rate has been virtually absent. Without the target in place we have never observed a background count at angles between 35° and 120° . If some of the concrete shields and lead around the Čerenkov counter are removed it is easily possible however to obtain background counts. These are usually small pulses in the photomultiplier and it is anticipated that with further study even these can be removed by applying a higher bias.

IV. CORRECTIONS TO DATA

The corrections usually applied to the raw scattering data have been excellently summarized by Lyman *et al.*¹¹ Many of these corrections are not needed in the present work, because the data to be presented are entirely of a relative kind. A precise absolute calibration of the scattering data has not been attempted up to the present time, although work is now under way to obtain absolute cross sections in gold.

Since we shall be concerned only with relative data, there is probably no need to take into account such small corrections as the radiative type of Schwinger¹⁷ which were calculated with Born approximation and depend very little on angle.

In order to avoid a variable loss of counts due to pileup, we have made an attempt to count approximately at the same rate at all angles so that a dead-time correction, if present, will be the same for all positions. Actually the dead time correction is negligible.

The largest corrections for multiple scattering are encountered in the case of the gold foils. For most measurements a foil 2 mils thick was used. In one run, to get more intensity at angles larger than 120° a four-mil foil was used. For the 2-mil foil the multiple scattering correction amounts to -0.3 percent at 35° , to -0.1 percent at 90° , and to -0.1 percent at 140° .

¹⁷ J. Schwinger, Phys. Rev. **75**, 898 (1949).

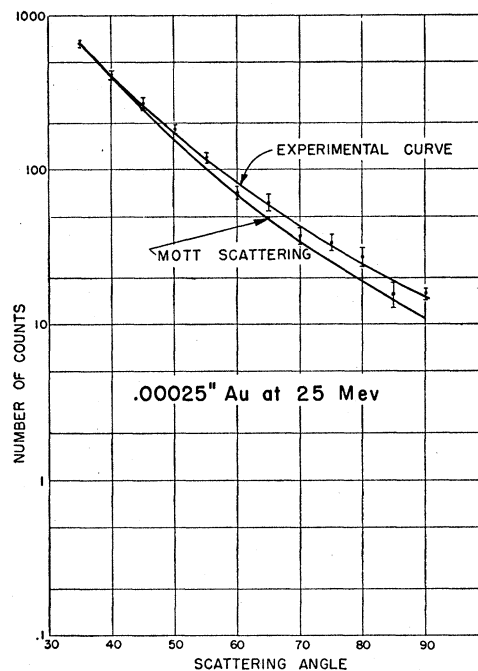


FIG. 8. The angular distribution of scattered electrons from a gold foil, $\frac{1}{4}$ -mil thick, at 25 Mev. The foil plane was at 45° with respect to the beam. The Mott curve for a point charge is shown. Arbitrary normalization is made at 35° .

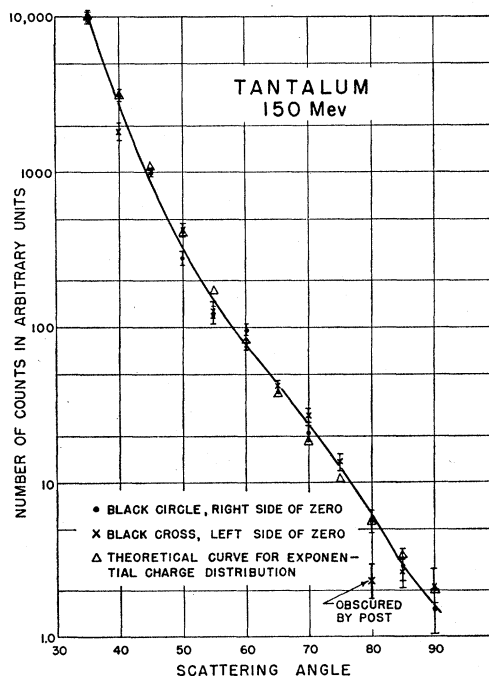


FIG. 9. The angular distribution of scattered electrons from a tantalum foil, 2.6-mil thick, at 150 Mev. The foil plane was at 30° relative to the beam direction. Curves on the left and right of zero are shown. A theoretical curve based on an exponential charge distribution is shown as well as the Feshbach point charge curve. All curves are normalized arbitrarily at 35° .

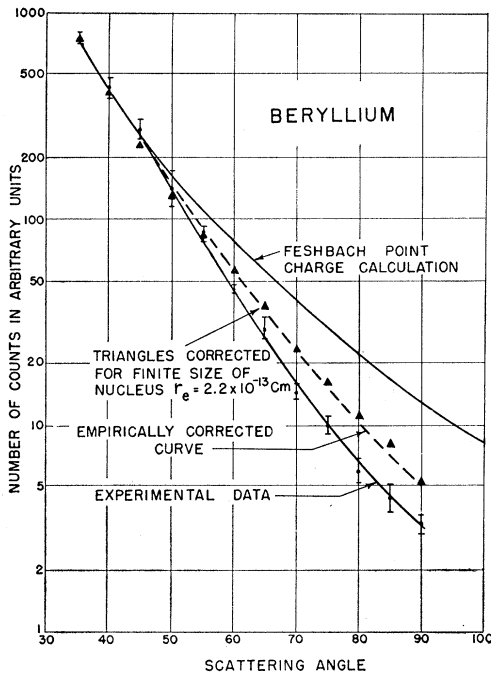


FIG. 10. The angular distribution of scattered electrons from a beryllium foil, 50-mils thick, at 125 Mev. The experimental curve has been corrected empirically for the broadening observed in the elastic curves at larger scattering angles. (See Fig. 6.) The dashed curve is the corrected curve. A theoretical curve based on the first Born approximation for an exponential charge distribution is shown. Also shown is the point charge calculation of Feshbach. Arbitrary normalization of all curves is made at 35° .

Thus, multiple scattering corrections in the target foil are unnecessary for the accuracy involved in this work. The multiple scattering in the aluminum windows is of the order of 0.4° and can be neglected since it is 4 times as small as the rms scattering angle in the gold foil. The beryllium 50-mil foil has an rms scattering angle of 0.6° which is negligible also.

The errors resulting from double (large-angle) scattering are estimated to be 0.15 percent at 90° for two mils of gold at 125 Mev and 0.01 percent at 150° under the same conditions. For 50 mils of Be at 125 Mev the errors are 1.5 percent at 150° and 0.04 percent at 90° . Hence, all double scattering corrections are ignored since they are very small effects.

The geometrical corrections for the aperture can be estimated from the effective aperture which is approximately 0.8 square inch at twelve inches. A calculation similar to that of Lyman *et al.* leads to corrections of a few tenths of a percent, which are thus negligible for our purposes.

The angular resolution of our scattering results depends on the size of the beam spot on the target foil and on the effective aperture of the entrance port of the analyzing magnet. Each of these contributions is about the same at the present time and each contributes about 2° , fairly independently of angles between 35° and 140° , for a target foil setting of 45° . Hence, our

angular acceptance width is about $\pm 4^\circ$, or a total of 8° . Structure in the scattering curves within such small angular ranges would not be resolved in our experiments. On the other hand, such fine structure is not expected.

Radiative straggling and electron-electron straggling affect the shape of the elastic-scattering peaks. Since in all the cases we have studied, with the exception of Be, the elastic profile is the same at all angles, no relative corrections for these effects need to be made. As a matter of fact, the same argument applies to the Schwinger correction.

With the exception of Be, all corrections are extremely small and will be ignored. In the case of Be (Fig. 6) the elastic profile changes as a function of angle, because of the combination of the recoil effect and the energy loss straggling in the target. Both effects are appreciable for Be. The correction has been taken into account empirically by measuring the areas under the elastic curves taken at various angles. At 90° the area is approximately 1.5 times the area at 35° when both curves are normalized to the same peak values. Hence, a correction of 50 percent is applied to the counting rate at 90° . At 35° the correction is zero, and a smooth curve has been drawn in Fig. 10 (the dashed line) to represent the corrected data at intermediate angles. Since the cross section varies rather violently with angle, the largest correction of 50 percent produces only a mild effect.

V. RESULTS

The relative angular distributions have been measured in Be, Au, and Pb at 125 Mev and in Ta at 150 Mev. In addition, as mentioned previously, check runs

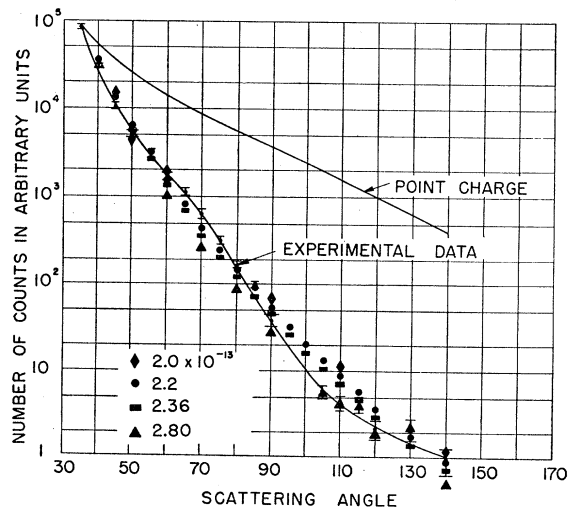


FIG. 11. The angular distribution of electrons scattered from a 2-mil gold foil at 125 Mev. The point charge calculation of Feshbach is indicated. Theoretical points based on the first Born approximation for exponential charge distributions are shown. Values of $\alpha = 2.0, 2.2, 2.36, 2.8 \times 10^{-13}$ cm are chosen to demonstrate the sensitivity of the angular distribution to change of radius. All curves are normalized arbitrarily at 35° .

were made on Be and Au at 25 Mev. The experimental curves are shown in Figs. 9, 10, 11, 12. The limits of errors indicated in the figures are entirely of statistical origin. In all cases except gold, the background counting rates were zero so that the present data represent the actual numbers taken in a run. In only one case, namely Au beyond 120° , was a small background observed in one of the counters. The other counter showed no background. The small background makes the data beyond 120° slightly less reliable than the other data.

Near 100° on the right side of zero it has not been possible to obtain data because of the presence of a steel post which is used as a support for the upper half of the scattering chamber. There is a similar post near 80° on the left-hand side of zero. In future experiments it will be possible to move the posts to other positions while taking data near these two angles.

In occasional runs we have noticed that after long periods of time the data do not check exactly. For example, after a couple of hours of running a point at 70° may change by 30 percent or so. Invariably the neighboring points will be down by the same factor. Thus, a slow drift in some part of the counting system or magnetic field appears at irregular times. The explanation of this effect is being sought. However, we do not feel that this effect is significant because the relative counting rates agree with those first obtained to better than 30 percent.

VI. ANALYSIS OF THE DATA

The experimental distributions lie far below the point charge calculations of Feshbach⁵ which are shown typically in Fig. 11. Within the resolution of the experimental data (points were taken every 5 degrees apart) there is no pronounced evidence of diffraction minima or maxima. These curves are in striking contrast to the beautiful curves of Cohen and Neidigh¹⁸ which show diffraction peaks in the scattering of 22-Mev protons.

The absence of pronounced diffraction peaks suggests that, from the viewpoint of the Born approximation, heavy nuclei do not have sharp boundaries. The accurate calculations of Yennie *et al.*¹⁰ confirm this suggestion in a qualitative way but not quantitatively. We shall sketch briefly some qualitative considerations provided by the Born approximation, merely in order to obtain a feeling for the meaning of the experimental results. In the discussion below we have used the exact calculations of Feshbach for the point charge and have multiplied the point charge curve by the appropriate form factors obtained from the first Born approximation^{2,4} for various assumed charge-density distributions.

¹⁸ B. L. Cohen and R. V. Neidigh, Phys. Rev. (to be published). We wish to thank Dr. A. M. Weinberg and Dr. B. L. Cohen for informing us of these results. See also J. W. Burkiq and B. T. Wright, Phys. Rev. **82**, 451 (1951).

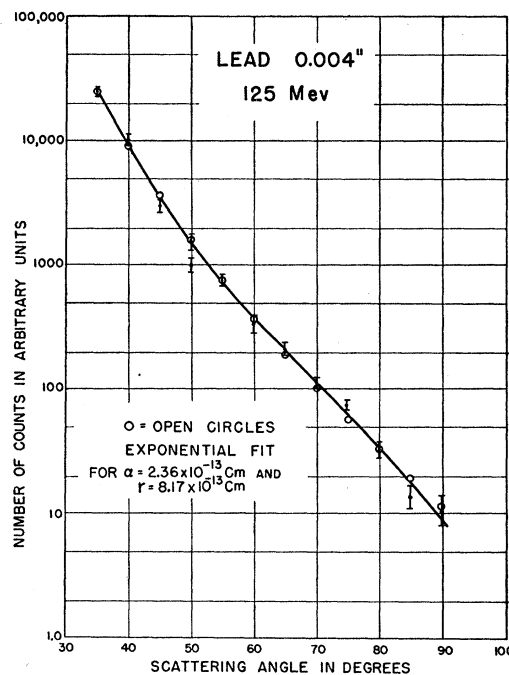


FIG. 12. The angular distribution of electrons scattered from a 4-mil lead foil at 125 Mev. A theoretical curve based on the first Born approximation for an exponential charge distribution is shown. Arbitrary normalization is made at 35° .

Among the types of charge-density (ρ) distributions tried¹⁹ were the following:

(A) exponential

$$\rho = \rho_0 e^{-r/\alpha}; \quad (4)$$

(B) "half-uniform and half-Gaussian"

$$\rho = \rho_1, \quad 0 \leq r \leq c; \quad \rho = \rho_1 \exp[-\frac{1}{2}(r-c)^2/d^2], \quad r \geq c; \quad (5)$$

(C) gaussian

$$\rho = \rho_2 \exp(-\frac{1}{2}r^2/r_0^2); \quad (6)$$

(D) uniform

$$\rho = \rho_3, \quad 0 \leq r \leq c; \quad \rho = 0, \quad r \geq c. \quad (7)$$

The ρ_0 , ρ_1 , ρ_2 , and ρ_3 are all constants with the dimensions of charge density. For these charge distributions the root-mean-square radii, calculated with the charge as the weighting factor are, respectively:

$$(A) \quad r_e = 3.46\alpha, \quad (8)$$

$$(B) \quad r_{ug} = 2.31c \quad \text{for } d=c, \quad (9)$$

$$(C) \quad r_g = 1.732r_0, \quad (10)$$

$$(D) \quad r_u = 0.775c. \quad (11)$$

In the following, we discuss the data obtained for the various elements.

¹⁹ See also L. I. Schiff (reference 8) for other charge distributions and relevant remarks. A slightly different approach from ours has been used in Schiff's paper.

Gold

The "best fit" with the experimental data was obtained for the exponential charge distribution with $\alpha = 2.3 \pm 0.3 \times 10^{-13}$ cm and $r_e = 7.95 \times 10^{-13}$ cm. The experimental data and the exponential fit are shown in Fig. 11. The half-uniform and half-Gaussian model provides a "best fit" which is somewhat inferior to the exponential fit and requires $c = 2.46 \times 10^{-13}$ cm and $r_{ug} = 5.7 \times 10^{-13}$ cm. This angular distribution is a poor fit at angles greater than 110° where it drops off too rapidly. The pure Gaussian model (C) is also not as good as the exponential but gives a best fit for $r_0 = 2.48 \times 10^{-13}$ cm with $r_g = 4.3 \times 10^{-13}$ cm. As in the last case the pure Gaussian drops off too rapidly beyond 115° . These rms radii are to be compared with the usual rms value of about 6.3×10^{-13} cm for gold and are of the correct order of magnitude.

The Born approximation is clearly quite poor for a uniform distribution of charge because of its true zeros. Therefore, no attempt will be made to use the Born approximation for this model. On the other hand, the exact calculations of Yennie *et al.*,¹⁰ carried out both for a uniform charge distribution and an exponential charge distribution, show that the exponential fits better because of the absence of diffraction structure, which does occur for the uniform distribution. In either event, the most important conclusion is that the exact theoretical curves reflect the very steep falloff of cross section with angle shown by the experiments. The large departures from a point charge are, therefore, satisfactorily demonstrated in theory, as well as experiment. The rather extreme exponential model, when treated exactly, appears to fit the experimental data (35° - 120°) quite well, but it is by no means ruled out that other less violent models with, e.g. Gaussian tails, might not do equally well. To see the qualitative effect of a small rounding off of the edge of a uniform charge distribution, a uniform model and Gaussian tail with parameter $d = 0.2c$ in Eq. (5) has been tried in Born approximation but does not remove the zeros. This model simply moves the zeros out a little towards larger angles. A uniform model with a small exponential tail has a similar behavior, as shown by Smith.⁷

Lead

The lead foil used in the experiments was an isotopic mixture in the natural proportions and was 4-mils thick. The experimental curve for 125 Mev is given in Fig. 12. It may be seen that the points are fitted quite well by a theoretical Born curve based on an exponential model. The theoretical curve is hardly distinguishable from the experimental curve. The radius obtained from the best exponential fit is $r_e = 8.17 \times 10^{-13}$ cm or $\alpha = 2.36 \times 10^{-13}$ cm. This value is slightly larger than the radius for gold in the ratio 1.03.

Tantalum

The experimental curve for 2.6 mils of tantalum at 150 Mev is given in Fig. 9. By fitting with an exponential charge distribution corresponding to $\alpha = 2.80 \pm 0.3 \times 10^{-13}$ cm or $r_e = 9.7 \times 10^{-13}$ cm, an excellent reproduction of the data is obtained. Again, as in lead, the theoretical Born points are scarcely distinguishable from the experimental ones. While the tantalum should have a radius slightly smaller than lead or gold according to the rule expressed by Eq. (3), the scattering data indicate a larger radius. Relative to lead the rms radius is 1.18 times as large. This result may possibly have some connection with the extremely large quadrupole moment of Ta.

Beryllium

Beryllium has been studied at 125 Mev. The results obtained with a 50-mil scattering target are shown in Fig. 10. The curve which has been empirically corrected for the change in elastic profile as a function of angle is shown as a dashed line in the figure. The point charge curve of Feshbach is shown in open circles. In the case of beryllium the Born approximation should be quite valid. The triangles represent the point charge curve as modified by the "best fit" form factor corresponding to an exponential charge distribution with $r_e = 2.2 \times 10^{-13}$ cm or $\alpha = 6.36 \times 10^{-14}$ cm. This radius is quite a bit smaller than the radii measured for heavy nuclei and is in good agreement with what might be expected from Eq. (3). In the case of such a small nucleus as Be, the form factor can be chosen quite arbitrarily to correspond either to the exponential, Gaussian, or uniform model, since all give essentially the same behavior. For example, the best fit for a uniformly charged model gives $r_u = 1.90 \times 10^{-13}$ cm and for a Gaussian model $r_g = 1.96 \times 10^{-13}$ cm.

VII. CONCLUSIONS

With the angular resolution attained in these experiments, the absence of diffraction maxima and minima in the observed scattering of 125- and 150-Mev electrons from Ta, Au, and Pb suggests tentatively the concept that these nuclei have charge distributions tapering off gradually from near the center to the outside. This conclusion is not definite at this time because both theory and experiment are in preliminary stages.

The differences between the nuclear diffraction patterns observed in the scattering of 22-Mev protons¹⁸ and the electron scattering results reported here may perhaps reflect the facts that nuclei interact with protons through short-range forces (also to a lesser extent through Coulomb forces) and are not transparent to protons of 22-Mev energy, while nuclei interact with electrons through long-range Coulomb forces and are transparent to electrons. Hence, the elastically-scattered protons interact effectively only with the outer edges of the

nucleus giving the impression of a sharp boundary. Electrons interact with the entire nuclear volume.

It might be wondered whether the peaked charge distribution suggested here could influence arguments concerning saturation of nuclear forces. A simple electrostatic calculation was carried out for the exponential charge distribution with $\alpha = 2.3 \times 10^{-13}$ cm for gold. The result obtained indicates that the Coulomb energy is changed by not more than a factor of two relative to that of the uniform distribution. Hence, on this score there will be no serious change regarding nuclear saturation.

It is recognized that the charge distribution in heavy nuclei tentatively suggested by this work differs rather seriously from the uniform model generally proposed. For this reason we are attempting to improve the accuracy of the experiments by increasing the angular resolution, energy resolution and stability of all parts of the apparatus.

ACKNOWLEDGMENTS

We wish to thank Mrs. P. Hanson, Mr. G. Masek, and assistant crew members for their kind and efficient help in running the accelerator. Miss E. Wiener and Mr. J. Fregeau have kindly assisted in taking some of the data. V. Prosper, E. Wright, B. Chambers, B. Stuart, F. Renga, and P. Abreu deserve our special

thanks for the skill they have shown in building and designing various parts of our scattering apparatus. Mr. R. H. Helm was of great assistance in designing the magnet support and in constructing the spectrometer. We appreciate the help of Drs. W. A. Fowler and W. Whaling of California Institute of Technology, who provided us with the drawings and advice needed in constructing the analyzing magnet, and Dr. I. Perlman of the University of California Radiation Laboratory, for lending us an alpha-particle calibration source. We are grateful to the Office of Naval Research which gave us early support in this project and particularly to Dr. Urner Liddel, Mr. F. Niemann, and Lt. M. S. Jones who helped us obtain the gun mount for this work. We wish to thank Dr. L. I. Schiff and Dr. W. E. Lamb, Jr., who have given us valuable advice in theoretical matters. Dr. E. Guth has read our work critically and has our special thanks for his comments. Drs. D. R. Yennie and D. G. Ravenhall and Mr. R. N. Wilson are to be thanked most cordially for their kindness in permitting us to use their results before publication. We acknowledge with thanks the recent support of the Office of Scientific Research of the Air Research and Development Command. Finally we are grateful for a grant received from the Research Corporation which enabled this project to obtain its start.